HHS Public Access

Author manuscript

Cell Rep. Author manuscript; available in PMC 2017 September 15.

Published in final edited form as:

Cell Rep. 2016 February 23; 14(7): 1662–1672. doi:10.1016/j.celrep.2016.01.030.

Atypical Protein Kinase C Dependent Polarized Cell Division is Required for Myocardial Trabeculation

Derek Passer[1,2,3], **Annebel van de Vrugt**[1,2], **Ayhan Atmanli**[1,2], and **Ibrahim Domian**[1,2,4,*]

[1]Cardiovascular Research Center, Massachusetts General Hospital, Charles River Plaza/CPZN 3200, 185 Cambridge Street, Boston, MA 02114-2790, USA

[2]Harvard Medical School, 250 Longwood Avenue, Boston, MA 02115, USA

[3]Department of Cellular and Integrative Physiology, University of Nebraska Medical Center, Omaha, NE 68198

[4]Harvard Stem Cell Institute, 1350 Massachusetts Avenue, Cambridge, MA 02138, USA

Abstract

A hallmark of cardiac development is the formation of myocardial trabeculations exclusively from the luminal surface of the primitive heart tube. Although a number of genetic defects in the endocardium and cardiac jelly disrupt myocardial trabeculation, the role of cell polarization remains unclear. Herein, we demonstrate that atypical protein kinase C iota (Prkci) and its interacting partners are localized primarily to the luminal side of myocardial cells of early murine embryonic hearts. A subset of these cells undergoes polarized cell division with the cell division plane perpendicular to the heart's lumen. Disruption of the cell polarity complex by targeted gene mutations results in aberrant mitotic spindle alignment, loss of polarized cardiomyocyte division, and loss of normal myocardial trabeculation. Collectively these results suggest that in response to inductive signals, Prkci and its downstream partners direct polarized cell division of luminal myocardial cells to drive trabeculation in the nascent heart.

Graphical abstract

*To whom correspondence should be addressed, domian@mgh.harvard.edu.

Author Contributions

D.L.P. and I.J.D. designed the experiments; D.L.P., A. V., and A. A.., performed and analyzed the experiments; D.L.P. and I.J.D wrote the manuscript; I.J.D. supervised the project.

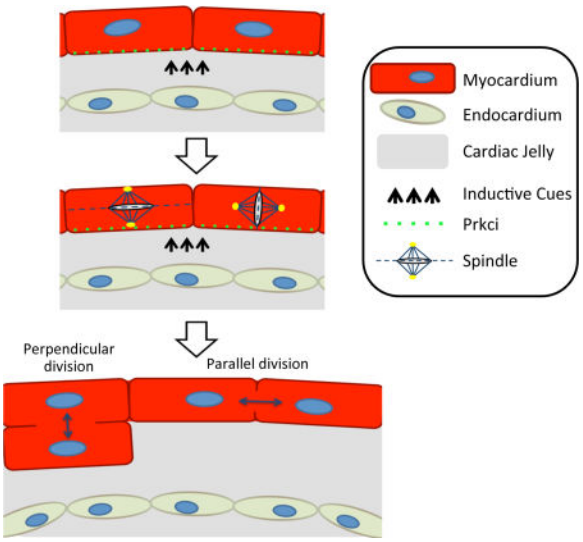

Introduction

During early mammalian cardiogenesis, progenitors of the cardiac crescent coalesce at the ventral midline to form the linear heart tube. At that point, the nascent heart is constituted of an inner endocardial cell layer separated from an outer myocardial layer by a complex of extracellular matrix (ECM) proteins termed the cardiac jelly(Moorman and Christoffels, 2003). By the end of cardiac looping on embryonic day (E) 9.0–9.5 in mouse, myocardial trabeculations orient toward the cardiac jelly and endocardial cells in the cardiac lumen (Manasek, 1968; von Gise and Pu, 2012). A number of genetic defects in the endocardium (Grego-Bessa et al., 2007; Liu et al., 2010) and cardiac jelly (Camenisch et al., 2000) have resulted in abnormal trabeculation of the early heart. Mutations in hyaluronan synthase-2 (Has2), for example, cause a loss of hyaluronic acid (HA) in the cardiac jelly, embryonic lethality at midgestation, and a lack of myocardial trabeculation (Camenisch et al., 2000). Likewise an increasing body of evidence suggests that oriented cell division is essential for establishing proper tissue architecture of the developing heart (Meilhac et al., 2004). Additionally late in heart development, oriented division of epicardial cells also controls epicardial cell migration and contribution to the myocardium (Wu et al., 2010). However the underlining molecular mechanisms which regulate proper spindle positioning in early cardiac development and trabecular formation remain poorly understood.

Cell polarity is an essential and highly conserved component of all eukaryotic cells during tissue development and refers to the polarized organization of cell membrane associated proteins as well as the asymmetric organization of organelles and cytoskeleton. (Bryant and Mostov, 2008). Recent studies in mammalian tissue culture cells suggest that polarized cell divisions rely on the unequal distribution and segregation of key polarity proteins during mitosis. These proteins govern the generation and proper axis alignment of differentiated cell types during organogenesis. During embryogenesis, polarity proteins regulate normal cellular physiology as well as tissue homeostasis and morphogenesis (Gonzalez, 2007; Knoblich, 2010; Martin-Belmonte and Perez-Moreno, 2012).

Cell polarity and spindle orientation are coupled through the Par polarity complex. The Par complex is composed of three proteins, Par3, Par6 and protein kinase C iota (Prkci), controls the cell polarity necessary for normal tissue generation and morphogenesis. First discovered during embryogenesis of C. elegans where polarity gene mutants caused loss of normal blastomore asymmetry and subsequent division cleavage planes (Watts et al., 1996). After establishment of the Par complex to one cell pole, Par3 interacts with the adapter protein Inscuteable (Insc in mammals) which binds directly to Pins (partner of Insc, homologue of vertebrate LGN/Gpsm2 and AGS3/Gpsm1). Pins then associates with the heterotrimeric G proteins ($G\alpha_i$) and NuMA. Critically, NuMA interacts directly with the cell spindle to control the orientation and of the spindle and the division plane of mitotic cells (Siller and Doe, 2009). Loss of function of any one of these genes results in an abnormal spindle orientation during polarized cell division leading to loss of tissue organization and failure of correct organogenesis (Silk et al., 2009).

This complex is conserved in multicellular organisms and is required for a number of polarized processes including asymmetric cell division (Betschinger et al., 2003), cell migration (Etienne-Manneville and Hall, 2003), and tight junction formation (Suzuki et al., 2001). In the neuroblast of C. elegans and *D. melanogaster*, Par cortical proteins align the mitotic spindle along defined axes (Siller and Doe, 2009). Likewise the zebrafish Heart and Soul gene encoding the atypical protein kinase C, directs the apical targeting of the zonula adherens. Mutations in this gene result in defects in heart tube assembly as well as the disruption of polarized epithelia in the retina, neural tube, and digestive tract (Horne-Badovinac et al., 2001). In mammals, the Par complex regulates stratification and differentiation of mammalian skin (Lechler and Fuchs, 2005), development of gut epithelium (Goulas et al., 2012), and eye lens formation (Sugiyama et al., 2009). Prkci complete null embryos die by day 9.5 and are morphologically abnormal lacking in any recognizable structures (Soloff et al., 2004). In the developing eye, a Prkci conditional knock out mouse line where the Prkci gene is inactivated in postmitotic photoreceptors causes severe laminar disorganization throughout the entire retina (Koike et al., 2005). In the immune system, disruption of Prkci in activated T cells caused severe defects in Th2 cytokine production. When challenged with an allergic stimulus, Prkci mutant mice had an impaired lung inflammatory response (Yang et al., 2009).

However despite an extensive body of literature documenting the importance of the distribution of cell polarity proteins and polarized cell division during organogenesis, the role of these cellular processes in normal cardiac development and trabecular formation has not been adequately examined in the developing heart. Herein we sought to address this gap in knowledge and define the role of the Par complex in directing cell polarization in early cardiac morphogenesis and trabecular formation.

Results

Par Complex components localize asymmetrically in luminal myocardial cells

We first examined whether polarity proteins are asymmetrically distributed in the linear heart tube, before the onset of trabeculation. Immunohistochemistry of E8.5 mouse embryos showed that both Prkci and its interacting partner Pard6g are localized mostly to the luminal

side of Troponin T (TnT) positive myocardial cells (Figure 1A). We then demonstrated that Prkci and Pard6g largely co-localize together with confocal microscopy (Figure 1B and 1C). Finally we confirmed that Pard6g and Prkci interact in a complex by co-immunoprecipitating Pard6g from embryonic lysates and immunoblotting for Prkci (Figure 1D). Next we systematically investigated whether other members of the polarity complex are also restricted to the luminal side of myocardial cells. As shown in Figures 1E–H, members of the polarity complex are spatially restricted chiefly to the luminal side of myocardial cells and are co-localized with other complex members. Finally we co-stained the complex members in the presence of both myocardial and endocardial markers (Figure 1I–K). These results are consistent with findings from multiple laboratories (Betschinger et al., 2003; Lechler and Fuchs, 2005; Shi et al., 2003) examining different organ systems and demonstrating that Par proteins interact as part of a cell polarization complex.

Luminal myocardial cells undergo polarized cell division in the early developing heart

Previously Le Garrec et al. demonstrated that myocardial cell division is oriented with a planar bias in embryonic mouse hearts (Le Garrec et al., 2013). We therefore examined E8.5 embryos (prior to the onset of trabeculation) to determine whether luminal myocardial cells displayed oriented cell division relative to the axis of polarity defined by the heart lumen. Prior work by Lechler and Fuchs established a standard methodology for the analysis of cell division angles relative to the basement membrane (Lechler and Fuchs, 2005). This approach also accounts for the three dimensional nature of divisions within tissue and excludes division outside the plane of the section or those occurring into the Z-plane. We adapted this approach to analyze the mitotic division plane of both early and late mitotic luminal ventricular cardiomyocytes relative to the cardiac lumen (Figure 2). To examine the plane of cell division of cardiomyocytes in the early stages of mitosis, E8.5 hearts were co-stained for TnT (cardiomyocyte marker), pericentrin (Pcnt, centromere marker), phospho-Histone H3 (pHH3, early mitosis marker), and DAPI (DNA stain). We were thereby able to define the spindle alignment and cell division plane of dividing cardiomyocytes relative to the cardiac lumen. As shown in Figures 2A and 2B, most early mitotic cell divisions occurred in a division plane parallel to the heart lumen. Of great interest however, a minority of mitotic cells had an alignment that was perpendicular to the lumen. pHH3 identifies predominantly late prophase, pro-metaphase, and metaphase cells. Since the early mitotic spindle can rotate during this window of time, we repeated the assay focusing solely on telophase cells in which both spindle poles can be readily identified within a thin section. Coalesced survivin immunostaining was used to identify the cleavage furrow of telophase cells and the reference line was drawn using the center of the segregating DNA mass when the spindle is in its committed orientation. As shown in Figures 2C and 2D, we again observed most late mitotic cell divisions occurring in a parallel division plane relative to the heart lumen, while a small population of dividing cells had an alignment that was perpendicular to the heart lumen. These results are reminiscent of cell division in murine skin cells where a shift from predominantly parallel/symmetric to perpendicular/asymmetric cell division coincides with epidermal stratification (Lechler and Fuchs, 2005).

Hyaluronic Acid (HA) in the cardiac jelly is required for Par complex localization

Our findings suggest that myocardial cells within the nascent heart are able to orient with respect to the lumen and raises the possibility that cardiac jelly mediates trabecular formation by directing the polarization and asymmetric cell division of luminal myocardial cells. Mutations in hyaluronan synthase-2 (Has2) result in loss of HA in the cardiac jelly, embryonic lethality at midgestation, and a lack of myocardial trabeculation (Camenisch et al., 2000). We therefore bred the Has2 null mouse line to create $Has2^{-/-}$ embryos (Camenisch et al., 2000). E8.5 $Has2^{-/-}$ embryos had delocalization of the Par complex (Figure 3A–D). In addition, the luminal myocardial cells of the mutant embryo had an apparently random pattern of cell division orientation during both early as well as late mitosis (Figure 3E–H). We also repeated this experiment in E8.0 $HAS2^{-/-}$ embryos and found a similar phenotype which shows a random pattern of cell division during both early and late mitosis (Figure S1). Although HA has been shown to bind to the CD44 receptor (Banerji et al., 1999), $CD44^{-/-}$ mice are viable with no trabeculation or other overt cardiovascular phenotype (Schmits et al., 1997). Nonetheless, we examined whether $CD44^{-/-}$ mice have defects in Par complex localization and spindle orientation in E8.5 embryos. As expected, Par complex and spindle orientation were not altered (Figure 3I–P). We therefore conclude that HA acts indirectly to control polarized cardiomyocyte division, potentially as a co-regulator facilitating endocardial signalling cues.

Prkci is required for polarized cell division, ventricular trabeculations, and embryonic viability

We then adopted a genetic approach to directly test whether cell polarity is required for trabecular formation (Figure 4). We bred a mouse line harboring a Prkci gene in which the essential exon 5 is flanked by loxP sites (Sugiyama et al., 2009) with a knock-in mouse line expressing Cre under the control of the mouse Nkx2.5 promoter (Moses et al., 2001). Myocardial deletion of the Prkci gene was embryonically lethal with no viable pups born (Figure S2). Gross analysis of the E10.5 knockout mouse heart revealed no grossly apparent morphological changes (Figure S3). Staining of E10.5 embryos for TnT, PECAM-1, and DAPI demonstrated a trabeculation defect with no trabeculations observed in the cardiac null mouse heart. In addition, the endocardium in the cardiac conditional null had no apparent morphological defects compared to the control embryo (Figure 4A–B). To further delineate the trabeculation defect, we imaged the heart with a combination of scanning electron microscopy (EM) and immunohistochemistry. Prkci cardiac null and control embryos were cryosectioned to the level of the mid cardiac cavity. The ultrastructure of the embryonic heart was then examined with scanning EM (Figure S4). In addition, adjacent cryosections were immunostained for TnT and the immunostained images were then overlaid with the scanning EM images (Figure 4C–D). As shown, this allowed us to demonstrate the absence of ventricular trabeculation in E10.5 conditional null hearts compared to the control. Next we show that the endocardium in the Prkci conditional null as well as the HAS2 null was normal in terms of marker expression by co-staining for the endothelial marker PECAM-1 (therefore staining endocardial cells) and the specific endocardial marker Nfatc1 (Figure 4E–G). We then confirmed that the trabecular markers BMP10, Cnx40, and PEG1 were down regulated in the Prkci mutant heart, however the

endocardial marker Nrg1, the compact myocardial marker N-myc, and the pan-cardiac markers Nkx2.5 and β-MHC were unchanged compared to controls (Figure 4H).

Prior work from the Pu laboratory demonstrated that the Nkx2.5-Cre mouse line can result in LoxP excision in the myocardium alone (in e.g. the Rosa26 locus) or in both the myocardium and endocardium (in e.g. the GATA4 locus) (Ma et al., 2008). To determine if this mouse line resulted in Prkci deletion in both the endocardium and the myocardium or in the myocardium alone, we immunostained the Prkci cardiac null embryos for Prkci. E8.5 Nkx-Cre/Prkci embryos and somitematched controls were cryosectioned and stained with Prkci, PECAM-1, TnT, and DAPI. As shown in Figure 4I–J, Prkci staining was absent from the mouse myocardium but present in the endocardium in cardiac null embryos, arguing for the specificity of the Prkci antibody and demonstrating the myocardial specific deletion of Prkci. In addition we also stained for Par complex members Pard6g and NuMA that we found to be delocalized within the myocardium of Prkci cardiac null hearts (Figure 4K–N).

Since Prkci is an integral component of the cell polarity machinery, we then examined mitotic division planes in Prkci cardiac null embryos during early and late stages of mitosis. As shown, deletion of Prkci resulted in a loss of perpendicular cell divisions relative to the heart's lumen during both early and late stages of mitosis (Figure 5A–D).

Previous work with a variety of cell types has shown that a scratch injury of a confluent monolayer of cells initiates directional cell migration and Golgi reorientation perpendicular to the wound (Etienne-Manneville and Hall, 2001). To determine if myocardial cells are capable of polarization during in vitro culture, we performed a scratch-wound assay on cardiomyocytes isolated from E12.5 mouse hearts. As shown in Figure 5E–F, in response to the scratch, embryonic cardiomyocytes at the leading edge reoriented their Golgi apparatus to face the wound. We then repeated the experiment with GF109203X, a small molecule inhibitor of atypical protein kinase C (Uberall et al., 1999). As shown in Figure 5G–H, this prevented Golgi reorientation towards the wound edge. These results show that embryonic cardiomyocytes cultured in vitro can be induced to polarize and that this polarization is dependent on atypical protein kinase C activity. Collectively our results demonstrate that Prkci is required for polarized Par complex, correct spindle orientation, and normal ventricular trabeculation.

NuMA is required for polarized cell division, ventricular trabeculations, and embryonic viability

NuMA acts downstream of Prkci and directly binds dynein to orient the cell spindle and mitotic division plane (Hawkins and Garriga, 1998; Silk et al., 2009). We therefore bred a conditional null NuMA mouse line (Silk et al., 2009) with the Nkx2.5-Cre mouse line to generate cardiac null NuMA mouse embryos (Figure 6). Myocardial specific deletion of the NuMA gene was embryonically lethal with no viable pups born (Figure S5). Gross analysis of the E10.5 NuMA cardiac null mouse heart revealed no revealed no abnormal changes to the heart's morphological structure (Figure S6). Immunohistochemical staining of E10.5 embryos for TnT and PECAM-1 demonstrated that the NuMA cardiac null, like the Prkci cardiac null, had a trabeculation defect while the endocardium appeared morphologically intact (Figure 6A–B). As expected, immunostaining of NuMA was absent from the

myocardium in the NuMA cardiac conditional null (Figure 6C–D). In contrast, Prkci localization was not significantly altered in the cardiac null, consistent with NuMA being downstream of Prkci (Figure 6E–F). Of note, we did not observe any significant differences in cardiomyocyte proliferation in cardiac null NuMA embryos or the other mutant embryos compared to controls (Figure 6G–H). We then examined whether early and late cardiomyocyte divisions are altered in the NuMA cardiac null. As shown, there was a marked reduction of perpendicular cell divisions and an increase in oblique and parallel cell divisions relative to the heart's lumen in both the early and late mitotic cardiomyocytes (Figure 7A–D). Accordingly, we conclude that NuMA directs trabecular formation by orienting the cell spindle and cell division plane perpendicular to the nascent heart's lumen.

Discussion

Myocardial trabeculation is a key morphologic event during cardiogenesis. Although a number of signaling molecules have been implicated in trabeculation (Grego-Bessa et al., 2007; Liu et al., 2010), the cellular processes that are required for trabecular formation are not fully understood in mammals. Herein we show that in mammals, polarized cell division is required for myocardial trabeculation. Key members of the Par complex, including Prkci, localize chiefly on the luminal side of myocardial cells and this requires a normal composition of the cardiac jelly. Depletion of HA from the cardiac jelly by HAS2 mutations results in loss of Par complex luminal localization. Consequently, this leads to an apparently random orientation of cardiomyocyte spindle orientation and division plane. Of importance however, mutations in the HA receptor CD44 do not affect Par complex localization or polarized cell division. These results argue that HA in the cardiac jelly does not directly control cell polarity but rather may modulate inductive signalling cues. This is analogous to how the ECM protein Fibrillin indirectly modulates TGF-β signalling during mammalian aortic development (Loeys et al., 2013).

Although our results demonstrate that Prkci dependent polarized cell division is required for trabecular formation during early cardiogenesis, they do not rule out the possibility that directed cell migration also contributes to this process. In zebrafish, directed cell migration appears to play a central role in trabecular formation (Liu et al., 2010). However important differences exist between zebrafish and mammals including the highly validated findings showing that cardiomyocyte proliferation occurs in the trabecular myocardium during development (Liu et al., 2010) and regeneration in zebrafish (Jopling et al., 2010), but predominantly in the compact myocardium in mammals (Buikema et al., 2013; Jeter and Cameron, 1971). Furthermore, the developing zebrafish heart is initially constituted from trabecular and embryonic primordial layers, with a third outermost cortical layer created during maturation into adulthood (Gupta and Poss, 2012).

In the skin, epidermal deletion of Prkci results in altered distribution of perpendicular versus planar cell division with an increase in perpendicular division (not planar or oblique divisions) (Niessen et al., 2013). In contrast Prkci deletion in the myocardium results in an increase in planar cell division. In both cases however, the loss of normal polarization results in abnormalities of the cellular differentiation program required for normal morphogenesis. These findings argue that in the heart, as in multiple other organ systems, the Par machinery

coordinates normal cellular differentiation by facilitating perpendicular cell division and promoting the differentiation of trabecular myocardium from compact myocardium.

A hallmark of tissue development is that the polarity of an individual cell is coupled to the organization of the organ as a whole (Horvitz and Herskowitz, 1992). Defining the processes whereby cellularpolarity is integrated with organogenesis is important not only for understanding normal development, but also for understanding the pathogenesis of human congenital diseases. Aberrant development of myocardial trabeculations for example can result in non-compaction cardiomyopathy (Luxan et al., 2013) and has been linked to aberrant signaling from the endocardium to the myocardium. Recapitulating the normal developmental processes that drive cell polarity and tissue organization will also be important in the regenerative approaches of cardiovascular medicine. The human heart has a limited endogenous regenerative capacity underscoring the need for new therapies. Recent work has opened the possibility for direct reprogramming of endogenous cardiac fibroblasts into functional myocardial cells (Qian et al., 2012; Song et al., 2012). An important challenge however is to not only expand the pool of functional cardiomyocytes, but also to promote their alignment and cellular integration with the native myocardium. Understanding the pathways that direct normal cardiomyocyte polarity in vivo will therefore be instrumental for the successful therapeutic application of cardiac regeneration.

Experimental Procedures

Immunohistochemistry

Embryos were fixed in 4% paraformaldehyde for 12–15 minutes and flash frozen in OCT, then stored at −80°C until cryosectioning. The sections were rinsed once in PBS for 10 minutes and blocked in 10% donkey serum in PBS/0.1% saponin. Primary antibodies were incubated with the sections overnight at 4°C. Following three 20 minute PBS washes, secondary antibodies with conjugated fluorochromes (Invitrogen) were added to each section for 60 min at 37°C. The sections were then washed three times for 20 minutes in PBS and then mounted using Prolong® antifade mounting medium (Invitrogen).

Primary Antibodies used were as follows: anti-Pard6g (sc-85097), anti-Prkci (sc-32020), anti-Pard3 (sc-168899), anti-gamma tubulin (sc-7396) (Santa Cruz Biotechnology). anti-giantin (ab24586), antiphospho histone H3 (ab10543), anti-pericentrin (ab4448), anti-Ki67 (15580) (abcam). anti-Troponin T (MA5-12960) (Pierce). anti-CD31 (550274), anti-NFATc1 (556602) (BD Pharmingen). anti-α actinin (A7811) (Sigma-Aldrich). anti-survivin (28085) (Cell Signaling). anti-MLC2v (10906-1-AP) (Proteintech). anti-NuMA was a kind gift from Duane A. Compton, Department of Biochemistry, Dartmouth Medical School.

Animal breeding

All mouse related studies were approved by the Subcommittee on Research Animal Care at Massachusetts General Hospital. To obtain mouse embryos that are cardiac deficient in Prkci or NuMA expression, we interbreed the previously described $Nkx2.5^{+/Cre}$ with either $Prkci^{Flox/Flox}$ (a kind gift from Shigeo Ohno at Yokohama City University) or $NuMA^{Flox/Flox}$ (a kind gift from Don W. Cleveland at UC San Diego School of Medicine),

to generate mice harbouring either Nkx2.5$^{+/Cre}$/Prkci$^{+/Flox}$ or Nkx2.5$^{+/Cre}$/NuMA$^{+/Flox}$ alleles. We bread these mice with mice carrying Prkci$^{Flox/Flox}$ alleles or NuMA$^{Flox/Flox}$ respectively. We also bred HAS2 null (Camenisch et al., 2000) and CD44 null(Protin et al., 1999) mice to create HAS2$^{-/-}$ and CD44$^{-/-}$ embryos respectively. This generated embryos that carry homozygous Prkci$^{Flox/Flox}$ alleles or NuMA$^{Flox/Flox}$ alleles and Nkx2.5$^{+/Cre}$. At days 8.5 and 10.5 post coitum, we euthanized the pregnant mother and dissected the embryos from the surrounding yolk sac and uterus. Embryos were subsequently imaged on a whole mount dissection microscope and their genotypes were determined by PCR analysis of tail biopsy samples.

Image analysis

Confocal 3D co-localization images were analyzed using PerkinElmer Volocity software. Image Z-stacks were first deconvolved using iterative restoration and then Manders and Pearson correlation coefficients computed with Volocity software. Scatter plots were generated from unenhanced, deconvolved images.

Electron microscopy

E10.5 Embryos were prepared and cryosectioned for EM scanning as previously described (Camenisch et al., 2000). Images of adjacent immunostained myocardium were then overlaid onto the EM images.

Co-immunoprecipitation

Total protein from E9.0 embryos was isolated using IP lysis buffer (Pierce, Rockford, IL). Co-immunoprecipitation was performed using the Pierce Co-Immunoprecipitation Kit following manufacturer's protocol. Protein-antibody mixture was incubated o/n at 4 °C with 5 μg antibody against Pard6g or rabbit isotype (Santa Cruz Biotechnology, Santa Cruz, CA). During the elution of the precipitated fraction, the samples were boiled for 5 min. at 100 °C in elution buffer with 6× loading buffer. Pull down samples and samples containing total lysate were loaded, separated, and transferred to a PVDF membrane using the Mini-Protean® Tetra system and the Mini Trans-Blot® Cell (BioRad, Hercules, CA). Membranes were blocked in 5% non-fat dry milk in 0,1% TBST and incubated with primary antibodies against Prkci (BD Biosciences, San Jose, CA). Subsequently, the membranes were probed with horseradish peroxidase-conjugated anti mouse (Jackson Immuno, West Grove, PA). The signal was visualized with SuperSignal West Pico Chemiluminescent Substrate (Pierce, Rockford, IL). ImageJ software was used for analysis.

qPCR

Total RNA of E10.5 wildtype and Prkci knockout hearts was isolated using the RNeasy Mini Kit (Qiagen, Valencia, CA) according manufacturer's protocol. cDNA was made using iScript™ cDNA Synthesis Kit (BioRad, Hercules, CA). Quantitive polymerase chain reaction was performed with SYBR GreenER™ qPCR SuperMix for ABI PRISM® (Invitrogen, Carlsbad, CA) and specific primers against β-actin, β-MHC, Nkx2.5, and the trabeculation markers BMP10, connexin40, and PEG1.

β-actin	F 5’-GGCTGTATTCCCCTCCATCG-3’
	R 5’-CCAGTTGGTAACAATGCCATGT-3’
β-MHC	F 5’-ACTGTCAACACTAAGAGGGTCA-3’
	R 5’-TTGGATGATTTGATCTTCCAGGG-3’
BMP10	F 5’-ATGGGGTCTCTGGTTCTGC-3’
	R 5’-CAATACCATCTTGCTCCGTGAA-3’
Connexin40	F 5’-GGTCCACAAGCACTCCACAG-3’
	R 5’-CTGAATGGTATCGCACCGGAA-3’
Nkx2.5	F 5’-GACAAAGCCGAGACGGATGG-3’
	R 5’-CTGTCGCTTGCACTTGTAGC-3’
PEG1	F 5’-TGACCCTGAGGTTCCATCGAG-3’
	R 5’-GCCGCAGAAGGGACTCTAC-3’

Ex vivo scratch assay

For ex vivo cardiac cell cultures, E12.5 hearts from wild-type mice were digested for 1 hour in collagenase A and B (1 mg/ml) and then 3 minutes in .25% Trypsin-EDTA to a obtain single-cell suspension. The cells were seeded onto a pre-gelatinized 96 well plate in mouse differentiation media. After 24hours, the cells were scratched in the presence of DMSO or GF 109203X (R&D systems) according to the previous described protocols (Etienne-Manneville and Hall, 2001; Liang et al., 2007) before fixation and immunostaining.

Measurements, quantification, and statistical analysis

qPCR results and the results related to the percentage of positive Ki67 and pHH3 cardiomyocytes in embryonic hearts are presented as mean ± SEM. Differences between groups were compared with a student's t test and one-way ANOVA with Dunnett post-hoc analysis respectively. A p value of <0.05 was considered statistically significant with * $P\leq0.05$, ** $P\leq0.01$, and *** $P\leq0.001$. The method for measurement of division angles has been described previously in (Lechler and Fuchs, 2005). Briefly, early stage mitotic cells were identified by pHH3 immunostaining and the centromere was identified by Pcnt immunostaining. Late-stage mitotic cells were identified by the presence of survivin at the midbody/cleavage furrow. Cells were scored only if both daughter nuclei surrounding the survivin staining could be unambiguously identified. Angles were measured by drawing a line through the centromere (early mitosis) or the centers of the two nuclei (late stage mitosis), and compared relative to the cardiomyocyte luminal membrane. Images were captured and measurements were quantified blind to genotype. To reduce any bias in data collection, all data from each group were not analyzed until all images were collected. n values indicated in each radial histogram indicate the number of luminal myocardial cells collected from 3–5 embryos. No statistical method was used to predetermine sample size, but data was collected from all available embryos of the indicated genotypes. Radial histograms were generated using Origin 9.0 software from data binned into 10° increments from 0 to 90°. For assessment of statistical significance of spindle orientation and angle of

cell division, a Chi-square test was calculated using two degrees of freedom. Data was categorized as follows: perpendicular (70–90°); planar (0–20°); oblique (20°–70°). As opposed to having equal 30° bins, we used these three categories based on the observation that most cardiomyocyte cell divisions fell into these ranges in wild type E8.5 hearts. Therefore a 20°–70° range represents a better deviation from normal than a 30°–60° range would. Data sets were compared by chi-square tests shown in Table 1 as previously described in (Williams et al., 2014). No statistical differences were found between age-matched littermates. All other graphs and statistical analyses (Student's t-tests and chi-square tests) were produced using GraphPad Prism.

Supplementary Material

Refer to Web version on PubMed Central for supplementary material.

Acknowledgments

We gratefully acknowledge Drs. Irving Zucker and Mark Lindsay for critical review of the manuscript and Dr. Jeffery Hill for his continued support throughout the project. This work was supported by grants from the National Institutes of Health/National Heart, Lung, and Blood Institute (NIH/NHLBI) [U01HL100408-01 and NIH/NHLBI 1K08 HL091209].

References

Banerji S, Ni J, Wang SX, Clasper S, Su J, Tammi R, Jones M, Jackson DG. LYVE-1, a new homologue of the CD44 glycoprotein, is a lymph-specific receptor for hyaluronan. The Journal of cell biology. 1999; 144:789–801. [PubMed: 10037799]

Betschinger J, Mechtler K, Knoblich JA. The Par complex directs asymmetric cell division by phosphorylating the cytoskeletal protein Lgl. Nature. 2003; 422:326–330. [PubMed: 12629552]

Bryant DM, Mostov KE. From cells to organs: building polarized tissue. Nature reviews Molecular cell biology. 2008; 9:887–901. [PubMed: 18946477]

Buikema JW, Mady AS, Mittal NV, Atmanli A, Caron L, Doevendans PA, Sluijter JP, Domian IJ. Wnt/beta-catenin signaling directs the regional expansion of first and second heart field-derived ventricular cardiomyocytes. Development. 2013; 140:4165–4176. [PubMed: 24026118]

Camenisch TD, Spicer AP, Brehm-Gibson T, Biesterfeldt J, Augustine ML, Calabro A Jr, Kubalak S, Klewer SE, McDonald JA. Disruption of hyaluronan synthase-2 abrogates normal cardiac morphogenesis and hyaluronan-mediated transformation of epithelium to mesenchyme. The Journal of clinical investigation. 2000; 106:349–360. [PubMed: 10930438]

Etienne-Manneville S, Hall A. Integrin-mediated activation of Cdc42 controls cell polarity in migrating astrocytes through PKCzeta. Cell. 2001; 106:489–498. [PubMed: 11525734]

Etienne-Manneville S, Hall A. Cdc42 regulates GSK-3beta and adenomatous polyposis coli to control cell polarity. Nature. 2003; 421:753–756. [PubMed: 12610628]

Gonzalez C. Spindle orientation, asymmetric division and tumour suppression in Drosophila stem cells. Nature reviews Genetics. 2007; 8:462–472.

Goulas S, Conder R, Knoblich JA. The Par complex and integrins direct asymmetric cell division in adult intestinal stem cells. Cell stem cell. 2012; 11:529–540. [PubMed: 23040479]

Grego-Bessa J, Luna-Zurita L, del Monte G, Bolos V, Melgar P, Arandilla A, Garratt AN, Zang H, Mukouyama YS, Chen H, et al. Notch signaling is essential for ventricular chamber development. Developmental cell. 2007; 12:415–429. [PubMed: 17336907]

Gupta V, Poss KD. Clonally dominant cardiomyocytes direct heart morphogenesis. Nature. 2012; 484:479–484. [PubMed: 22538609]

Hawkins N, Garriga G. Asymmetric cell division: from A to Z. Genes & development. 1998; 12:3625–3638. [PubMed: 9851969]

Horne-Badovinac S, Lin D, Waldron S, Schwarz M, Mbamalu G, Pawson T, Jan Y, Stainier DY, Abdelilah-Seyfried S. Positional cloning of heart and soul reveals multiple roles for PKC lambda in zebrafish organogenesis. Current biology : CB. 2001; 11:1492–1502. [PubMed: 11591316]

Horvitz HR, Herskowitz I. Mechanisms of asymmetric cell division: two Bs or not two Bs, that is the question. Cell. 1992; 68:237–255. [PubMed: 1733500]

Jeter JR Jr, Cameron IL. Cell proliferation patterns during cytodifferentiation in embryonic chick tissues: liver, heart and erythrocytes. Journal of embryology and experimental morphology. 1971; 25:405–422. [PubMed: 5556983]

Jopling C, Sleep E, Raya M, Marti M, Raya A, Izpisua Belmonte JC. Zebrafish heart regeneration occurs by cardiomyocyte dedifferentiation and proliferation. Nature. 2010; 464:606–609. [PubMed: 20336145]

Knoblich JA. Asymmetric cell division: recent developments and their implications for tumour biology. Nature reviews Molecular cell biology. 2010; 11:849–860. [PubMed: 21102610]

Koike C, Nishida A, Akimoto K, Nakaya MA, Noda T, Ohno S, Furukawa T. Function of atypical protein kinase C lambda in differentiating photoreceptors is required for proper lamination of mouse retina. The Journal of neuroscience : the official journal of the Society for Neuroscience. 2005; 25:10290–10298. [PubMed: 16267237]

Le Garrec JF, Ragni CV, Pop S, Dufour A, Olivo-Marin JC, Buckingham ME, Meilhac SM. Quantitative analysis of polarity in 3D reveals local cell coordination in the embryonic mouse heart. Development. 2013; 140:395–404. [PubMed: 23250213]

Lechler T, Fuchs E. Asymmetric cell divisions promote stratification and differentiation of mammalian skin. Nature. 2005; 437:275–280. [PubMed: 16094321]

Liang CC, Park AY, Guan JL. In vitro scratch assay: a convenient and inexpensive method for analysis of cell migration in vitro. Nature protocols. 2007; 2:329–333. [PubMed: 17406593]

Liu J, Bressan M, Hassel D, Huisken J, Staudt D, Kikuchi K, Poss KD, Mikawa T, Stainier DY. A dual role for ErbB2 signaling in cardiac trabeculation. Development. 2010; 137:3867–3875. [PubMed: 20978078]

Loeys BL, Mortier G, Dietz HC. Bone lessons from Marfan syndrome and related disorders: fibrillin, TGF-B and BMP at the balance of too long and too short. Pediatric endocrinology reviews : PER. 2013; 10(Suppl 2):417–423. [PubMed: 23858625]

Luxan G, Casanova JC, Martinez-Poveda B, Prados B, D'Amato G, MacGrogan D, Gonzalez-Rajal A, Dobarro D, Torroja C, Martinez F, et al. Mutations in the NOTCH pathway regulator MIB1 cause left ventricular noncompaction cardiomyopathy. Nature medicine. 2013; 19:193–201.

Ma Q, Zhou B, Pu WT. Reassessment of Isl1 and Nkx2-5 cardiac fate maps using a Gata4-based reporter of Cre activity. Developmental biology. 2008; 323:98–104. [PubMed: 18775691]

Manasek FJ. Embryonic development of the heart. I. A light and electron microscopic study of myocardial development in the early chick embryo. Journal of morphology. 1968; 125:329–365. [PubMed: 5678904]

Martin-Belmonte F, Perez-Moreno M. Epithelial cell polarity, stem cells and cancer. Nature reviews Cancer. 2012; 12:23–38.

Meilhac SM, Esner M, Kerszberg M, Moss JE, Buckingham ME. Oriented clonal cell growth in the developing mouse myocardium underlies cardiac morphogenesis. The Journal of cell biology. 2004; 164:97–109. [PubMed: 14709543]

Moorman AF, Christoffels VM. Cardiac chamber formation: development, genes, and evolution. Physiological reviews. 2003; 83:1223–1267. [PubMed: 14506305]

Moses KA, DeMayo F, Braun RM, Reecy JL, Schwartz RJ. Embryonic expression of an Nkx2-5/Cre gene using ROSA26 reporter mice. Genesis. 2001; 31:176–180. [PubMed: 11783008]

Niessen MT, Scott J, Zielinski JG, Vorhagen S, Sotiropoulou PA, Blanpain C, Leitges M, Niessen CM. aPKClambda controls epidermal homeostasis and stem cell fate through regulation of division orientation. The Journal of cell biology. 2013; 202:887–900. [PubMed: 24019538]

Protin U, Schweighoffer T, Jochum W, Hilberg F. CD44-deficient mice develop normally with changes in subpopulations and recirculation of lymphocyte subsets. Journal of immunology. 1999; 163:4917–4923.

Qian L, Huang Y, Spencer CI, Foley A, Vedantham V, Liu L, Conway SJ, Fu JD, Srivastava D. In vivo reprogramming of murine cardiac fibroblasts into induced cardiomyocytes. Nature. 2012; 485:593–598. [PubMed: 22522929]

Schmits R, Filmus J, Gerwin N, Senaldi G, Kiefer F, Kundig T, Wakeham A, Shahinian A, Catzavelos C, Rak J, et al. CD44 regulates hematopoietic progenitor distribution, granuloma formation, and tumorigenicity. Blood. 1997; 90:2217–2233. [PubMed: 9310473]

Shi SH, Jan LY, Jan YN. Hippocampal neuronal polarity specified by spatially localized mPar3/mPar6 and PI 3-kinase activity. Cell. 2003; 112:63–75. [PubMed: 12526794]

Silk AD, Holland AJ, Cleveland DW. Requirements for NuMA in maintenance and establishment of mammalian spindle poles. The Journal of cell biology. 2009; 184:677–690. [PubMed: 19255246]

Siller KH, Doe CQ. Spindle orientation during asymmetric cell division. Nature cell biology. 2009; 11:365–374. [PubMed: 19337318]

Soloff RS, Katayama C, Lin MY, Feramisco JR, Hedrick SM. Targeted deletion of protein kinase C lambda reveals a distribution of functions between the two atypical protein kinase C isoforms. Journal of immunology. 2004; 173:3250–3260.

Song K, Nam YJ, Luo X, Qi X, Tan W, Huang GN, Acharya A, Smith CL, Tallquist MD, Neilson EG, et al. Heart repair by reprogramming non-myocytes with cardiac transcription factors. Nature. 2012; 485:599–604. [PubMed: 22660318]

Sugiyama Y, Akimoto K, Robinson ML, Ohno S, Quinlan RA. A cell polarity protein aPKClambda is required for eye lens formation and growth. Developmental biology. 2009; 336:246–256. [PubMed: 19835853]

Suzuki A, Yamanaka T, Hirose T, Manabe N, Mizuno K, Shimizu M, Akimoto K, Izumi Y, Ohnishi T, Ohno S. Atypical protein kinase C is involved in the evolutionarily conserved par protein complex and plays a critical role in establishing epithelia-specific junctional structures. The Journal of cell biology. 2001; 152:1183–1196. [PubMed: 11257119]

Uberall F, Hellbert K, Kampfer S, Maly K, Villunger A, Spitaler M, Mwanjewe J, Baier-Bitterlich G, Baier G, Grunicke HH. Evidence that atypical protein kinase C-lambda and atypical protein kinase C-zeta participate in Ras-mediated reorganization of the F-actin cytoskeleton. The Journal of cell biology. 1999; 144:413–425. [PubMed: 9971737]

von Gise A, Pu WT. Endocardial and epicardial epithelial to mesenchymal transitions in heart development and disease. Circulation research. 2012; 110:1628–1645. [PubMed: 22679138]

Watts JL, Etemad-Moghadam B, Guo S, Boyd L, Draper BW, Mello CC, Priess JR, Kemphues KJ. par-6, a gene involved in the establishment of asymmetry in early C. elegans embryos, mediates the asymmetric localization of PAR-3. Development. 1996; 122:3133–3140. [PubMed: 8898226]

Williams SE, Ratliff LA, Postiglione MP, Knoblich JA, Fuchs E. Par3-mInsc and Galphai3 cooperate to promote oriented epidermal cell divisions through LGN. Nature cell biology. 2014; 16:758–769. [PubMed: 25016959]

Wu M, Smith CL, Hall JA, Lee I, Luby-Phelps K, Tallquist MD. Epicardial spindle orientation controls cell entry into the myocardium. Developmental cell. 2010; 19:114–125. [PubMed: 20643355]

Yang JQ, Leitges M, Duran A, Diaz-Meco MT, Moscat J. Loss of PKC lambda/iota impairs Th2 establishment and allergic airway inflammation in vivo. Proceedings of the National Academy of Sciences of the United States of America. 2009; 106:1099–1104. [PubMed: 19144923]

Highlights

- Prkci localizes primarily to luminal side of cardiomyocytes in the early embryonic hearts.
- A subset of these cells undergoes polarized cell division perpendicular to the lumen.
- Cell polarization requires a normal composition of the cardiac jelly.
- Deletion of Par complex components results in loss of myocardial trabeculation.

Prkci dependent cell polarization is required for the ventricular trabeculation of the mammalian heart. Passer et al. find that Prkci and and its interacting partners polarize luminal myocardial cells and is requied for cardiac trabeculation in the nascent heart.

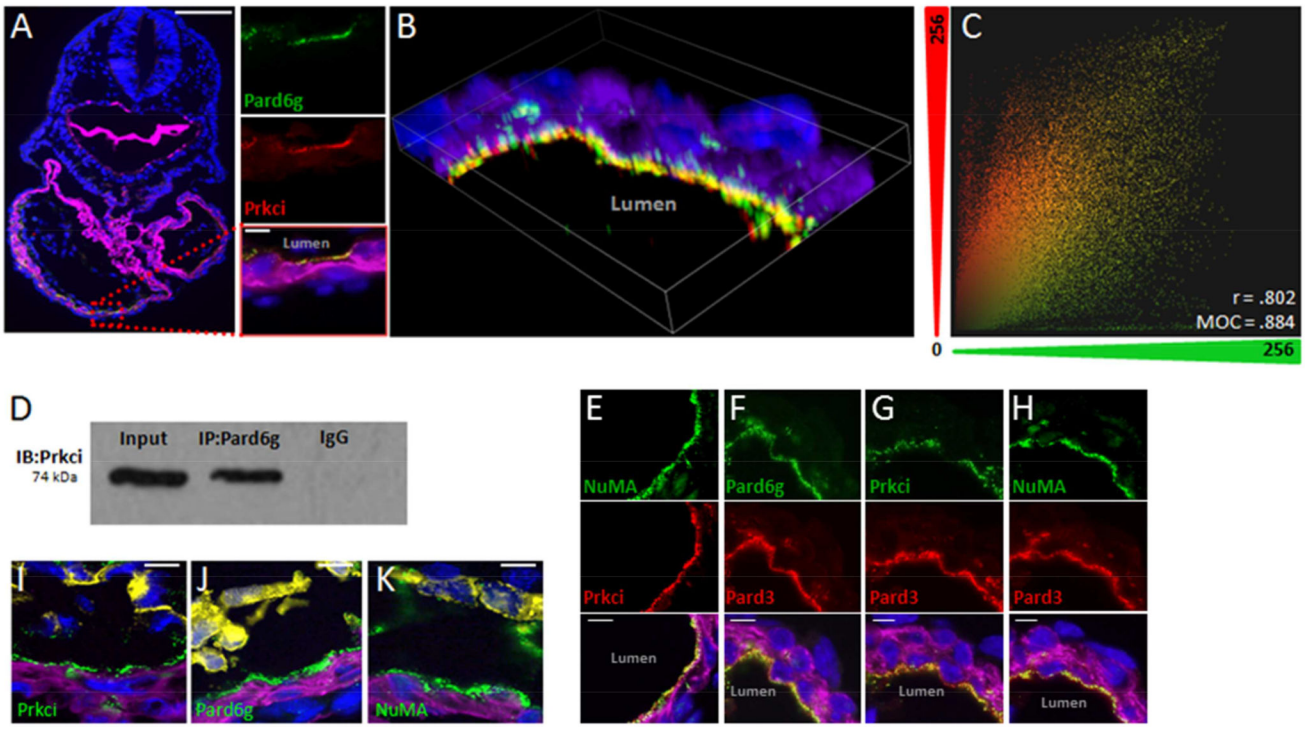

Figure 1. Luminal localization of Par complex members in early embryonic hearts

A. E8.5 embryonic hearts co-stained for Pard6g (green), Prkci (red). **B**. Confocal microscopy showing co-localization of Pard6g and Prkci. **C.** A 2D scatter plot of fluorescence intensities in the green (x, Prkci) and red (y, Pard6g) channels was reconstructed from the 3-D image and the Manders Overlap Coefficient (MOC) and Pearson Correlation Coefficient (r) were calculated. This demonstrates significant co-localization of the red and green channels in three dimensions. **D.** Embryonic lysates were immunoprecipitated with anti-Pard6g antibody and then immunoblotted with anti-Prkci. **E–H.** Par complex members co-stained green or red as indicated. **I–K** Par complex members (green) co-stained with PECAM-1 (yellow, outlining the endocardium). TnT (purple) and DNA (DAPI, blue). Scale bars: 100μm zoom out, 10μm elsewhere.

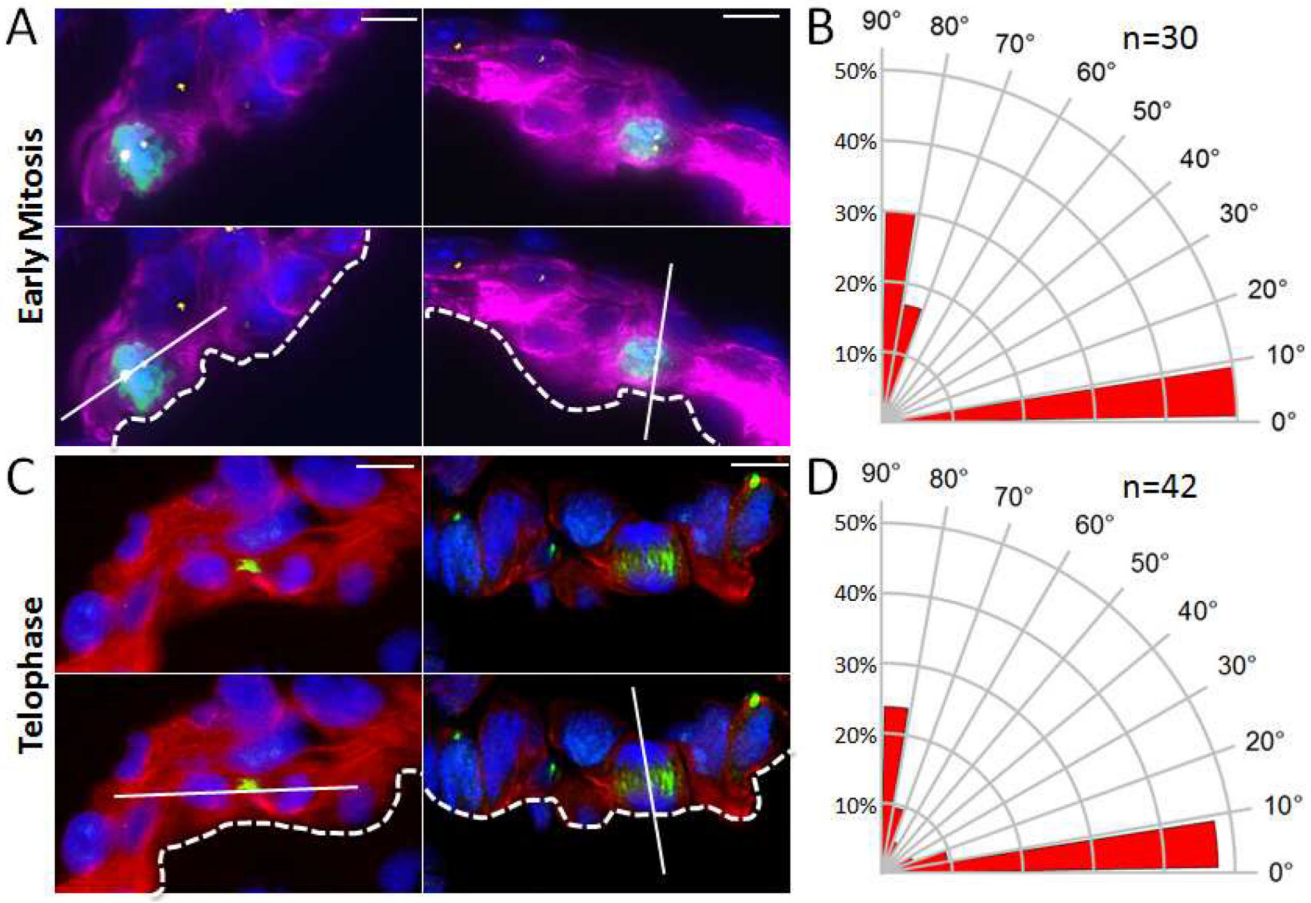

Figure 2. Polarized cell division in luminal myocardial cells of E8.5 hearts

A. Top panels: Representative images of early mitotic luminal cardiomyocytes in E8.5 wild-type hearts co-stained for pHH3 (green), Pcnt (yellow), TnT (purple), and DAPI (blue). Lower panels: Superimposed axis of cell division (solid line) relative to the cardiac lumen (dashed line). **B**. Radial histogram depicting the orientation of cardiomyocyte divisions in early-stage mitotic cells from E8.5 wild-type hearts. **C**. Top panels: Representative images of luminal telophase cardiomyocytes in E8.5 wild-type hearts co-stained for survivin (green), TnT (red), and DAPI (blue). Lower panels: Superimposed axis of cell division (solid line) relative to the cardiac lumen (dashed line). **D.** Radial histogram depicting the orientation of cardiomyocyte divisions in late-stage mitotic cells from E8.5 wild-type hearts. Scale bars: 10μm.

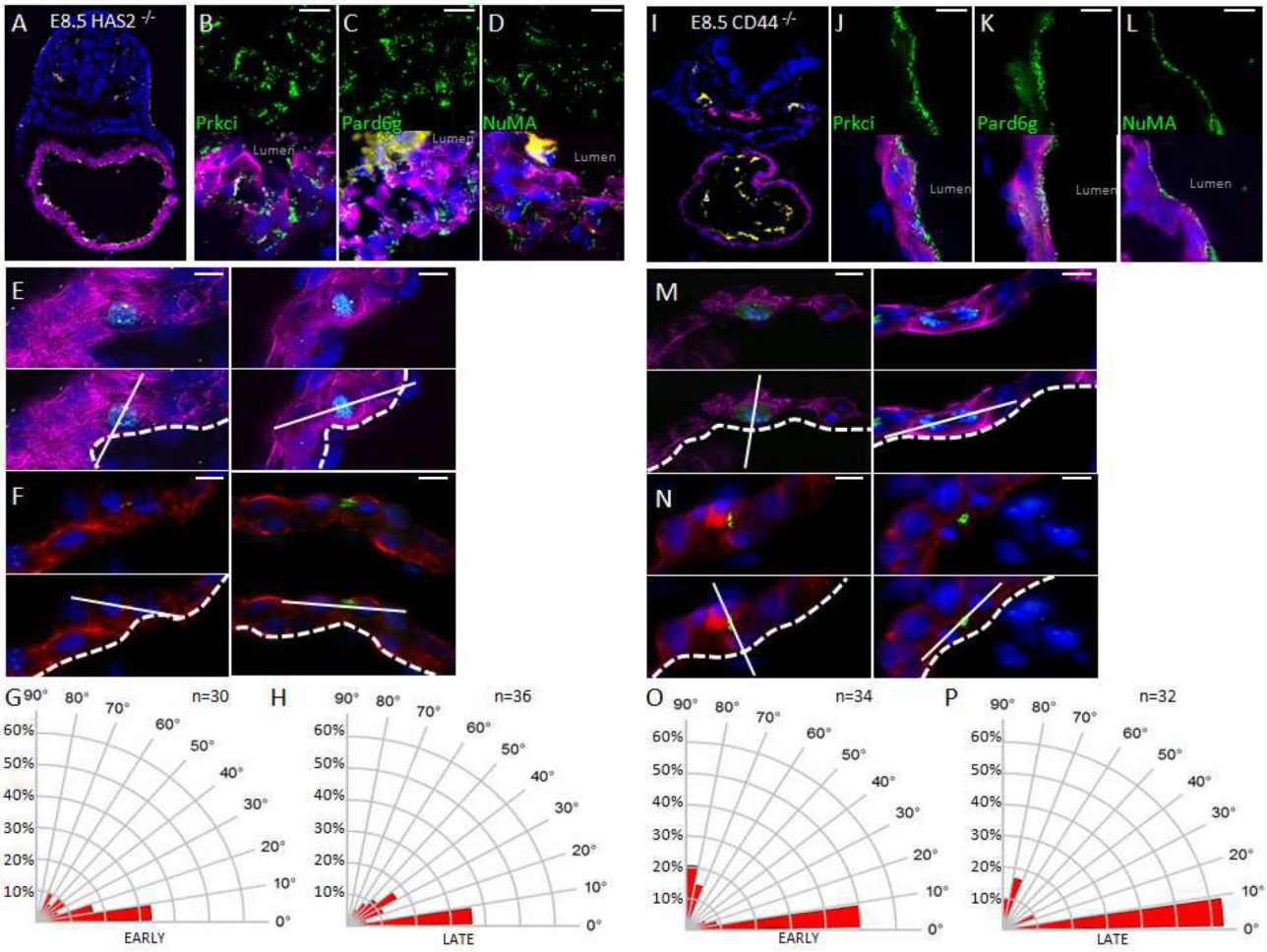

Figure 3. HA in the cardiac jelly is required for polarized cell division in E8.5 mouse hearts

A. E8.5 HAS2$^{-/-}$ embryo co-stained for TnT (purple), PECAM-1 (yellow), and DAPI (blue). **B–D**. E8.5 HAS2$^{-/-}$ embryonic hearts stained in green for Prkci (**B**), Pard6g (**C**), or NuMA (**D**). **E.** Top panels: Representative images of early mitotic luminal cardiomyocytes in E8.5 HAS2$^{-/-}$ hearts co-stained for pHH3 (green), Pcnt (yellow), TnT (purple), and DAPI (blue). Lower panels: Superimposed axis of cell division (solid line) relative to the cardiac lumen (dashed line). **F**. Top panels: Representative images of luminal telophase cardiomyocytes in E8.5 HAS2$^{-/-}$ hearts co-stained for survivin (green), TnT (red), and DAPI (blue). Lower panels: Superimposed axis of cell division (solid line) relative to the cardiac lumen (dashed line). **G**. Radial histogram depicting the orientation of cardiomyocyte divisions in early-stage mitotic cells from E8.5 HAS2$^{-/-}$ hearts. **H.** Radial histogram depicting the orientation of cardiomyocyte divisions in late-stage mitotic cells from E8.5 HAS2$^{-/-}$ hearts. **I.** E8.5 CD44$^{-/-}$ embryo co-stained for TnT (purple), PECAM-1 (yellow), and DAPI (blue). **J–L**. E8.5 CD44$^{-/-}$ embryonic hearts stained in green for Prkci (**J**), Pard6g (**K**), or NuMA (**L**). **M.** Top panels: Representative images of early mitotic luminal cardiomyocytes in E8.5 CD44$^{-/-}$ hearts co-stained for pHH3 (green), Pcnt (yellow), TnT (purple), and DAPI (blue). Lower panels: Superimposed axis of cell division (solid line) relative to the cardiac lumen (dashed line). **N**. Top panels: Representative images of luminal

telophase cardiomyocytes in E8.5 CD44$^{-/-}$ hearts co-stained for survivin (green), TnT (red), and DAPI (blue). Lower panels: Superimposed axis of cell division (solid line) relative to the cardiac lumen (dashed line). **O**. Radial histogram depicting the orientation of cardiomyocyte divisions in early-stage mitotic cells from E8.5 CD44$^{-/-}$ hearts. **P.** Radial histogram depicting the orientation of cardiomyocyte divisions in late-stage mitotic cells from E8.5 CD44$^{-/-}$ hearts. Scale bars: 100μm zoom out, 10μm elsewhere else. *P* values (P≤0.001 for early and late mitosis) determined by a chi-square test in **G&H** and **O&P** for determining significance of the difference between HAS2 null and wildtype cells. Chi-square *P* values related to **G&H** and **O&P** are in Table S1. *n* values in **G&H** and **O&P** represent the number of cells analyzed from 3 to 5 independent animals.

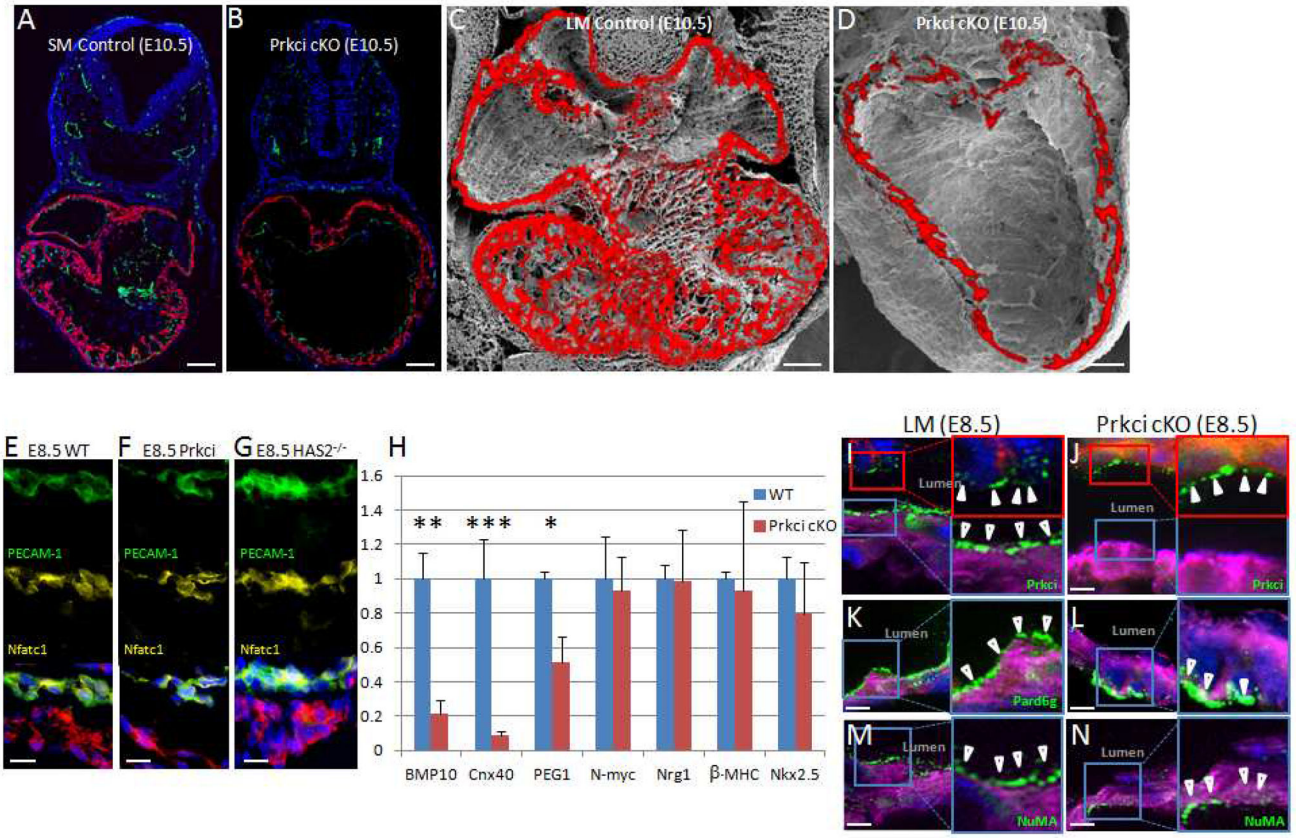

Figure 4. Prkci is required for normal ventricular trabeculation

A&B. E10.5 somite matched (SM) control (**A**) and Prkci cardiac conditional knockout (cKO) (**B**) embryos immunostained for PECAM-1 (yellow), TnT (red), DAPI (blue). **C&D.** Scanning EM of cryosectioned E10.5 littermate (LM) heart (**C**) or Prkci cKO (**D**). Scanning EM images are overlaid with adjacent TnT immunostained sections. **E–G.** Indicated KO embryos co-stained for endocardial markers PECAM-1 (green) and Nfatc1 (yellow), along with the ventricular marker MLC2v (red). **H.** RT-PCR analysis in E10.5 WT and Prkci mutant hearts. **I–N.** Immunostaining of littermate control (**I, K, M**) or Prkci cardiac null (**J, L, N**) E8.5 embryos stained for Prkci (**I&J**), Pard6g (**K&L**), or NuMA (**M&N**). Specified polarity protein (green), DAPI (blue), PECAM-1 (red), and TnT (purple). Closed arrowheads point to faint polarity protein staining on the endocardium. Open arrowheads point to luminal polarity protein staining on myocardium. Scale bars: 100μm zoom out and 10μm elsewhere else. *P* values (*P≤0.05, ** P≤0.01, and *** P≤0.001.) determined by a Student's *t*-tests in **H**.

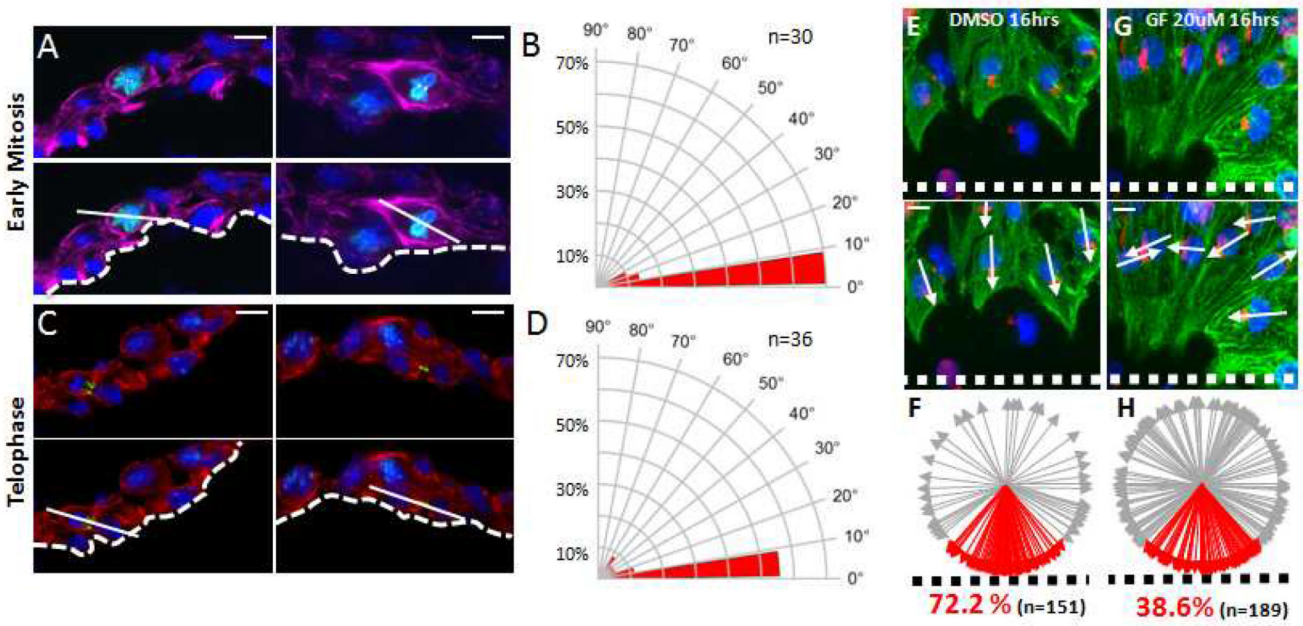

Figure 5. Prkci is required for cardiomyocyte polarization

A. Top panels: Representative images of early mitotic luminal cardiomyocytes in E8.5 Prkci cardiac null hearts co-stained for pHH3 (green), Pcnt (yellow), TnT (purple), and DAPI (blue). Lower panels: Superimposed axis of cell division (solid line) relative to the cardiac lumen (dashed line). **B.** Radial histogram depicting the orientation of cardiomyocyte divisions in early-stage mitotic cells from E8.5 Prkci cardiac null hearts. **C.** Top panels: Representative images of luminal telophase cardiomyocytes in E8.5 Prkci cardiac null hearts co-stained for survivin (green), TnT (red), and DAPI (blue). Lower panels: Superimposed axis of cell division (solid line) relative to the cardiac lumen (dashed line). **D.** Radial histogram depicting the orientation of cardiomyocyte divisions in late-stage mitotic cells from E8.5 Prkci cardiac null hearts. **E.** Representative example of Golgi reorientation 16hrs after scratch injury of a confluent layer of E12.5 embryonic cardiomyocytes cultured in vitro. **F**. Percentage of leading edge cardiomyocytes with the Golgi in the 90° sector facing the scratch injury. **G**. Representative example of Golgi reorientation 16hrs after wounding in vitro E12.5 cardiomyocytes in the presence of GF109203X. **H**. Percentage of leading edge cardiomyocytes with the Golgi in the forward-facing 90° sector in the presence GF109203X. Alphaactinin (green), Golgi (red), DAPI (blue). Scale bars: 10μm. *P* values (P≤0.001 for both early and late cell division) determined by a chi-square test in **B&D** for determining significance of the difference between cardiac null and wildtype cells. Chi-square *P* values related to **B&D** are in Table S1. *n* values in **B&D** represent the number of cells analyzed from 3 to 5 independent animals.

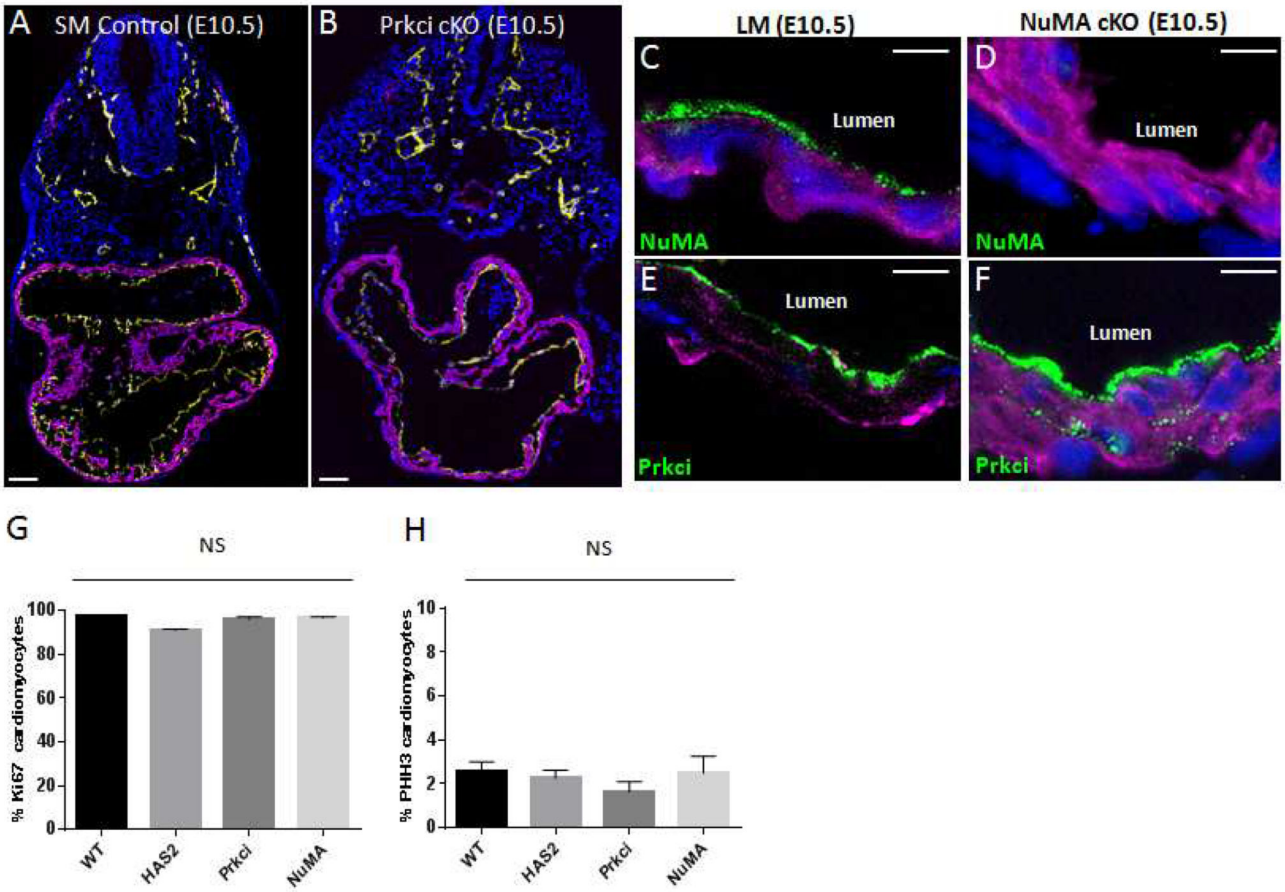

Figure 6. NuMA is required for cell polarization and normal ventricular trabeculation

A&B. E10.5 somite matched (SM) control (**A**) and NuMA cKO (**B**) embryos immunostained for PECAM-1 (yellow), TnT (purple), DAPI (blue). **C–F**. Immunostaining of a littermate control (**C&E**) or NuMA cardiac null (**D&F**) embryo stained for NuMA (**C&D**) or Prkci (**E&F**). Specified polarity protein (green), DAPI (blue), and TnT (purple). **G&H**. Quantification of Ki67 (**G**) or pHH3 (**H**) positive cardiomyocytes in specified E8.5 mutant embryos. Scale bars: 100μm zoom out and 10μm elsewhere else. NS, not significant.

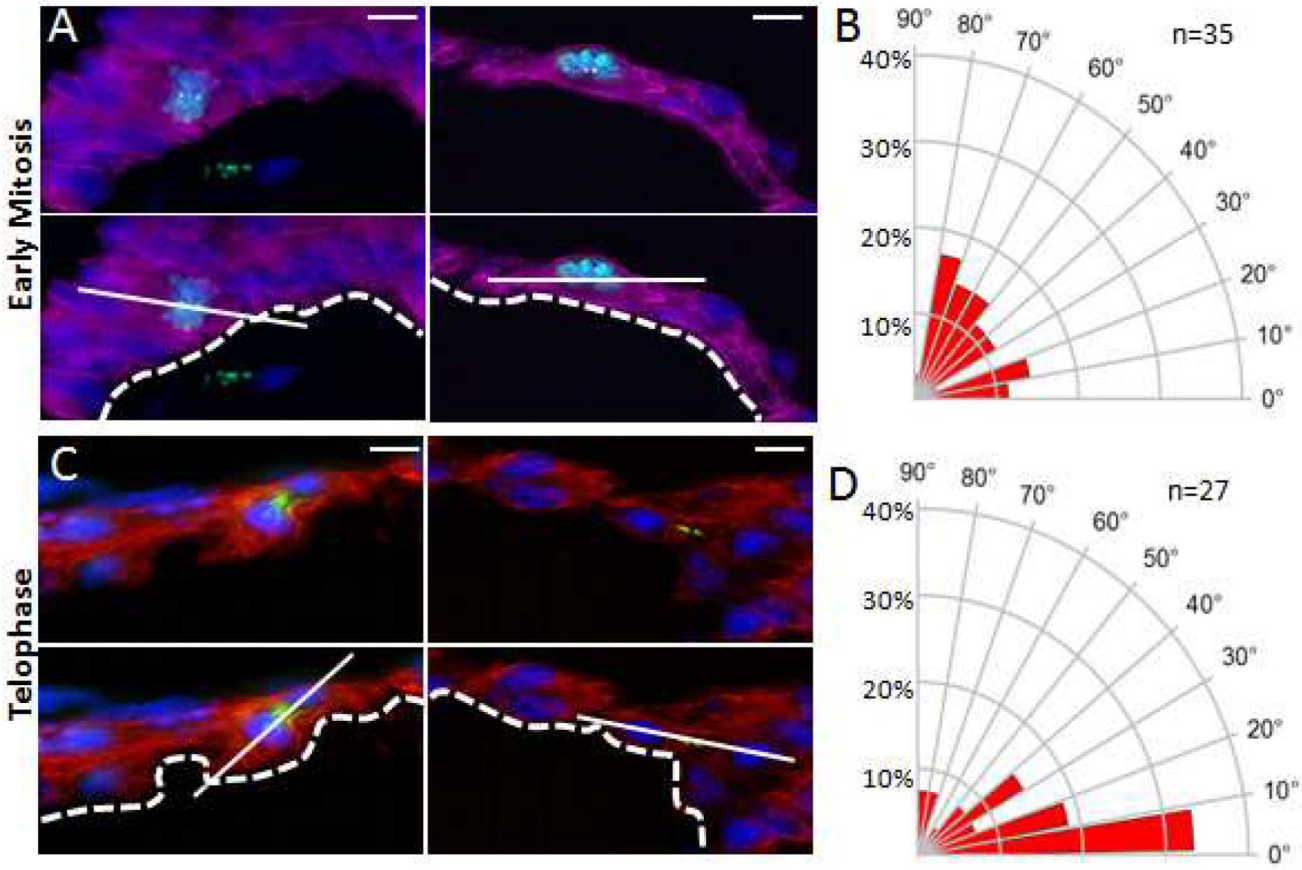

Figure 7. Luminal Cardiomyocyte Division Angles in E8.5 NuMA Cardiac Null Mouse Ventricles

A. Top panels: Representative images of early mitotic luminal cardiomyocytes in E8.5 NuMA cardiac null hearts co-stained for pHH3 (green), Pcnt (yellow), TnT (purple), and DAPI (blue). Lower panels: Superimposed axis of cell division (solid line) relative to the cardiac lumen (dashed line). **B.** Radial histogram depicting the orientation of cardiomyocyte divisions in early-stage mitotic cells from E8.5 NuMA cardiac null hearts. **C.** Top panels: Representative images of luminal telophase cardiomyocytes in E8.5 NuMA cardiac null hearts co-stained for survivin (green), TnT (red), and DAPI (blue). Lower panels: Superimposed axis of cell division (solid line) relative to the cardiac lumen (dashed line). **D.** Radial histogram depicting the orientation of cardiomyocyte divisions in late-stage mitotic cells from E8.5 NuMA cKO hearts. Scale bars: 10μm. *P* values (P≤0.01 for early and P≤0.001 for late) determined by a chi-square test in **B&D** for determining significance of the difference between cardiac null and wildtype cells. Chi-square *P* values related to **B&D** are in Table S1. *n* values in **B&D** represent the number of cells analyzed from 3 to 5 independent animals.